

Interrupted Growth to Manipulate Phase Separation in DIP:C60 Organic Semiconductor Blends

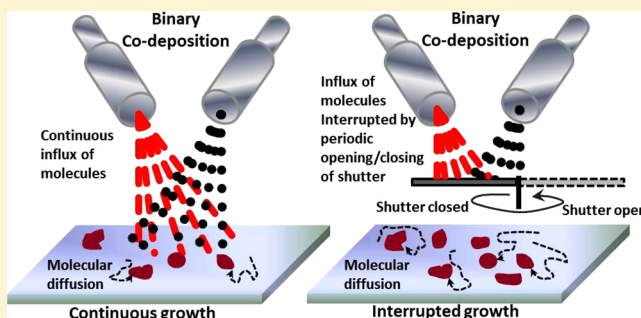
Rupak Banerjee,^{*,†} Alexander Hinderhofer,[‡] Michael Weinmann,[‡] Berthold Reisz,[‡] Christopher Lorch,[‡] Alexander Gerlach,[‡] Martin Oettel,[‡] and Frank Schreiber[‡]

[†]Department of Physics, Indian Institute of Technology Gandhinagar, Palaj, Gandhinagar 382355, India

[‡]Institut für Angewandte Physik, Universität Tübingen, Auf der Morgenstelle 10, 72076, Tübingen, Germany

S Supporting Information

ABSTRACT: We studied the influence of periodic growth interruptions during codeposition of diindenoperylene (DIP) and buckminsterfullerene (C60) in an equimolar mixing ratio. DIP and C60 are known to phase-separate when codeposited, but the details and, in particular, the length scales depend on kinetic factors. Using X-ray scattering and atomic force microscopy, we demonstrate that the phase separation mechanism is in fact influenced by growth interruptions, with more pronounced effects if the deposition rates are low. For high deposition rates, growth interruptions have no appreciable effect. We discuss our proof-of-concept investigation in the context of the relevant processes and their time scales.



INTRODUCTION

Organic semiconductors have shown great potential for electronic and optoelectronic device applications, with potential advantages being ease of preparation, better tunability, and higher oscillator strength for certain transitions.^{1,2} In addition to single-component systems studied mostly for transistor applications, multicomponent systems and, in particular, donor–acceptor combinations are in focus for photovoltaics and light-emitting devices.³ One strategy is to employ donor–acceptor blends, such as obtained by codeposition of the two materials. The structural complexities and the rich phase behavior in such blends^{4–9} make detailed quantitative investigations imperative, but also rather complicated.¹⁰ This includes both the molecular structure as well as the mesoscopic morphology, since, e.g., the length scale of potential phase separation, compared to length scales of electronic processes such as charge carrier diffusion lengths, can be crucial for device performance.^{11–15} Optimizing structure and morphology for device performance is a nontrivial multicomponent problem, so it is not easy to pin it down to any one particular structural or morphological feature because often the device properties show complex relationship to their inherent structure. Nevertheless, it seems to be accepted in the community that a certain level of roughness of the interface between the donor and the acceptor is favorable to enhance chances for exciton dissociation and thus organic photovoltaic device efficiency.^{16,17} Our present results provide one additional handle as to how to tailor these structural and morphological features.

Growth phenomena are nontrivial to comprehend and sometimes very difficult to account for quantitatively since

these are essentially nonequilibrium processes where new material continually impinges on the substrate and causes hindrance to equilibration of growth.^{10,18–21} Concepts based on the minimization of energy alone are insufficient to account for thin organic crystalline structures grown on inert substrates using vapor sublimation since the structure formation involves many kinetic processes, e.g. diffusion, nucleation, adsorption, desorption, and dissociation.^{22–24} These concepts are neglected in purely energetic considerations of growth. However, understanding of growth mechanisms involves essentially all of these processes which are inherently connected to the dynamic aspects of thin film growth. The diversity of the growth phenomena for thin films is huge, and often a smart model has to be invoked for a quantitative explanation of the parameters involved.^{18,25} Changes in the preparation conditions of thin film growth, for instance, substrate temperature and deposition rate, often lead to significantly different structural and morphological features. These complexities are already found for pure materials. The case when materials are codeposited (almost invariably leading to intermixing at different levels) becomes even more difficult to understand. Previous studies have categorized three case scenarios⁴ essentially determined by the adsorbate–adsorbate interaction and the temperature: (a) a solid solution constituting of a stochastic mixture of the mixing materials, (b) a new periodically ordered complex which is different from the

Received: September 28, 2017

Revised: December 21, 2017

Published: December 22, 2017



mixing materials, and (c) phase segregation of the mixing materials into separate domains of individual material. In a thin film, the occurrence of these mixing scenarios might also depend on the layer height above the substrate. An appreciable effect of steric compatibility is also observed in such mixed blends giving rise to an even broader range of scenarios than parts a–c above.⁵ Using complementary X-ray scattering²⁶ and atomic force microscopy measurements, several studies have revealed how the length scale of phase separation proceeds and how different growth parameters may be tuned to alter the growth and consequently the structural properties.^{6,27–30}

The combination of diindenoperylene (DIP) and buckminsterfullerene (C60) (see Figure 1, parts a and b, for molecular

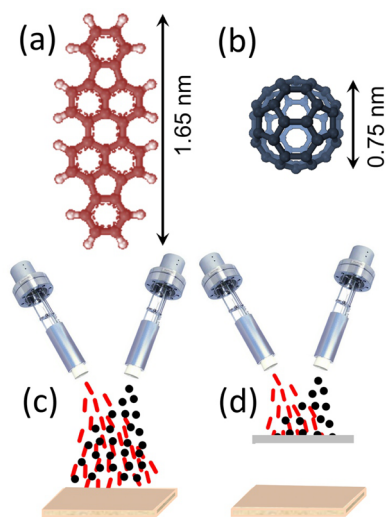


Figure 1. Molecular structure of the materials used in coevaporation: (a) diindenoperylene (DIP, $C_{32}H_{16}$) and (b) buckminsterfullerene (C60). The growth methods are depicted schematically in parts c and d. For continuous growth (c), the molecule flux is uninterrupted. For interrupted growth (d), the flux is interrupted sequentially by a motorized shutter to allow for enhanced diffusion of the aggregates before they encounter the incoming flux of molecules again.

structures of DIP and C60, respectively) as a donor–acceptor combination in the active area of the OPV cells have demonstrated good solar cell performance, most notably a very high fill factor.^{14,15} This material combination is phase-separating under equilibrium conditions and allows for the fundamental investigation into growth and morphology of such phase-separating mixtures. Essential parameters that define the growth scenario of such blends are the incoming flux of the molecules and the relative time of diffusion, within a layer or to adjacent layers, the molecules need to become attached to each other in an energetically favorable configuration. Phase separation over potentially large length scales is obviously a rather dramatic example. The competition between flux and diffusion determines the growth, and altering the influx process obviously addresses this. Making the flux rate time-dependent, with interruptions being the most dramatic version, is a less investigated path and will be explored in this work.

For the chosen system, DIP:C60 with composition 1:1 grown on a native oxide coated silicon (nSiO), previous studies^{6,27,28} lead to the following findings. Initial film growth is relatively smooth, in contrast to the growth of pure substances which is island-like from the start. Demixing of the two components is presumably absent for the first layers but

becomes more pronounced with increasing film thickness as evidenced by depth-resolved studies of DIP and C60 crystallite sizes.⁶ This coherent crystallite size is strongly temperature-dependent and is increasing with larger temperatures, especially for the DIP crystallites.²⁷ The DIP crystallite size is also very susceptible to the flux rate: at a substrate temperature of 100 °C and a flux rate of 1.5 Å/min, the crystallite size which was 355 Å decreases to about 119 Å for a flux rate of 14 Å/min at the same substrate temperature.²⁷

In this paper, we demonstrate, as a proof-of-concept, that by sequential interruption of the growth process (see Figure 1, parts c and d, and also Figure S1 in the Supporting Information for schematic depiction of continuous and interrupted growth), it is possible to change the growth process and the resulting structure and morphology of the thin film and to address the question of characteristic time scales in the demixing process of the binary system. While the protocol of interrupted growth is relatively new for organic blends, for inorganic heterostructures, it is already a common practice to use interruptions during growth^{31–34} as has been demonstrated in the case of (Al,Ga)As/GaAs, GaAs(001) heterostructure grown by molecular beam epitaxy. Very high quality quantum well structures could be fabricated by growth interruptions.³¹ It was observed that growth interruptions lead to drastic reduction of the effective roughness of top interface of the heterostructures involved,³³ the surface exhibited many 2D islands elongated along a particular growth direction and a ragged step configuration.³⁴ It is observed that the interruption is most effective when the growth rates are already slow, and for faster growth rates the influence of interruption on the growth is minimal. Comparison to typical island formation times of islands in films grown with the pure materials DIP and C60 shows that a typical demixing time is much shorter. It is argued that by tuning the interruption protocol more detailed information about layer thickness-dependent demixing times should be obtainable.

EXPERIMENTAL SECTION

DIP was obtained from the University of Stuttgart and purified twice via temperature gradient sublimation before use. C60 was purchased from CreaPhys and used without further purification. The films were prepared using a customized ultrahigh vacuum chamber operating at a base pressure of $<10^{-9}$ mbar following concepts described in earlier reports.^{4,20} The thickness was monitored using a water-cooled quartz crystal microbalance (QCM). The thickness of the film was calibrated by measuring the QCM thickness and corrected by a factor which compensates for the sticking and desorption coefficient. The actual thicknesses of the film were confirmed by performing X-ray reflectivity measurements. Silicon covered with native oxide (nSiO) was used as a substrate and cleaned with acetone, isopropanol, and purified water before deposition. The substrates were heated up to 500 °C before deposition. All deposition involving a systematic variation in the growth rate as well as interruption was carried out at a temperature of 24 °C. X-ray scattering measurements were carried out at the ID10 beamline of the ESRF. The chosen energy was 14 keV (corresponding to a wavelength of 0.886 Å). X-ray reflectivity (XRR), which gives the information on the out-of-plane structure, thickness and roughness of the film by measuring the reflectivity as a function of the normal component (q_z) of the momentum transfer vector (\mathbf{q}) was performed in the coplanar geometry such that the incident angle and exit angles were

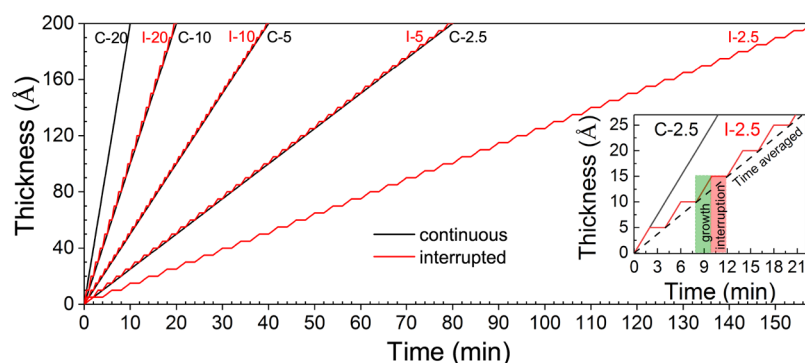


Figure 2. Deposition procedure for codeposited thin films under investigation. The sample designation is C/I - r_{dep} for continuous/interrupted growth at the deposition rate r_{dep} in Å/min over the entire film deposition. The inset clearly shows the systematic interruption employed during growth for one such r_{dep} of 2.5 Å/min. For the interrupted growth, the duration of interruption was chosen to be equal to the duration of deposition such that the time averaged deposition rate r_{avg} over the entire growth process (shown by the broken line), was half of the actual deposition rate r_{dep} .

always same. Grazing incidence X-ray diffraction (GIXD), which gives information on the in-plane crystallinity of the thin film by measuring the intensity as a function of the in-plane component (q_{xy}) of \mathbf{q} , was performed by fixing the incident angle to 0.12° such that the signal originates predominantly from the top organic layer. The experiment was performed with a Cyberstar scintillation counter with a beam size of 0.1 mm horizontal \times 0.02 mm vertical. Vertical detector slit sizes for XRR were 0.1 mm, for GIXD the horizontal slit sizes were 0.5 mm with a sample detector distance of 800 mm. The critical angle of DIP, C60 and mixed films at this energy is around 0.1° and the critical angle of Si is 0.13° . With an angle of incidence of 0.12° we probed the whole organic film without penetrating the Si substrate. All measurements were done ex-situ after the films were deposited. Data acquisition times were optimized to allow enough statistics without any overexposure leading to radiation damage. Typical XRR measurements took around 20 min and typical GID took around 60 min. The Bragg peaks in the GIXD data were fitted with Gaussians (refer to Figure S2 in Supporting Information) to obtain the full width at half-maximum (fwhm) of the peaks. Scherrer's equation ($d_{coh} = 2\pi \times K/\text{fwhm}$ with $K = 0.94$ for spherical crystallites and fwhm being the full width at half-maximum of the particular peak) was used to calculate d_{coh} . Possible effects of the instrumental broadening were not included, hence the estimated values are lower limits only. Atomic force microscopy (AFM) was performed using the JPK Nanoscope II instrument (JPK Instruments AG, Berlin, Germany), in the intermittent tapping mode under ambient conditions. The resonant frequency of the cantilever used was 300 kHz. The pyramidal-shaped tip was made of silicon and had a tip radius of less than 10 nm. The images were collected at a scan rate of 0.5 lines per second. The Gwyddion image processing software was used to refine and analyze the AFM images.

RESULTS AND DISCUSSION

It is expected that if the routine growth processes are altered systematically, it will have an influence on the resulting structure and morphology of the samples. Here, we focus on the attempt to manipulate the phase separation via interruption in the growth process. In an earlier report, we demonstrated how the other experimental control parameters affect the structure and morphology of equimolar films of DIP:C60.²⁸ Since the growth of such thin films has kinetic limitations, we investigated this behavior by changing the deposition rates

(r_{dep}) and the interruption time (t_{int}) during the growth process. We define the average rate (r_{avg}) as the time averaged deposition rates for the growth of the entire thin film (see Figure 2 for different r_{dep} and inset for a comparison between continuous and interrupted growth together with the assignment of the time-averaged rate of growth). In order to gain a total film thickness of 200 Å at different deposition rates while keeping the number of interruptions constant, the duration of deposition and interruption periods were adjusted accordingly.

XRR data are plotted in Figure 3. It is observed that the films grown at a higher r_{dep} have more pronounced oscillations than the ones with much lower r_{dep} . However, we see a signature of a broad Bragg reflection in the films with lower r_{dep} compared to the ones at higher r_{dep} . The broad reflection is a signature of crystalline domains of the pure materials, meaning that the phase separation is more pronounced in films with a stronger Bragg reflection. This is in accordance with the general behavior of organic thin film growth for most pristine molecules³⁵ that slower growth rates actually enhance the crystallinity of the sample but at the same time make it rougher. Usually, higher r_{dep} leads to smoother films with decreased crystallinity. The same trend is visible even for codeposited films although the degree of crystallinity is much less in a mixed system of DIP:C60 when compared to growth behavior of pure DIP or pentacene (PEN) molecules.

In addition, upon a comparison of the films deposited either continuously or by systematic interruptions we observe that the crystallinity is enhanced for all the different r_{dep} in the case of interrupted growth. The effect is more pronounced for the low r_{dep} films than the ones for the high r_{dep} films. This is a clear signature that the interruptions actually enhance the out-of-plane structure of the mixed films. The low r_{dep} rate films already show some crystallinity during continuous growth and the enhancement is more prominent for the synchronized interrupted growth at the same r_{dep} . Importantly, we observe that if the film is already crystalline during continuous growth (Figure 3a), there is further enhancement in the crystallinity during interrupted growth (Figure 3b). As is expected, the roughness decreases in accordance with the increase in the fraction of crystallinity of the films. It is noted that the out-of-plane crystallinity does not vary monotonously with the decreasing flux rate from C-5 to C-2.5 (continuously growing films) and we also see this in the in-plane crystallite size in Figure 5 estimated from the GIXD. However, in all the other films grown continuously at higher rates or grown with

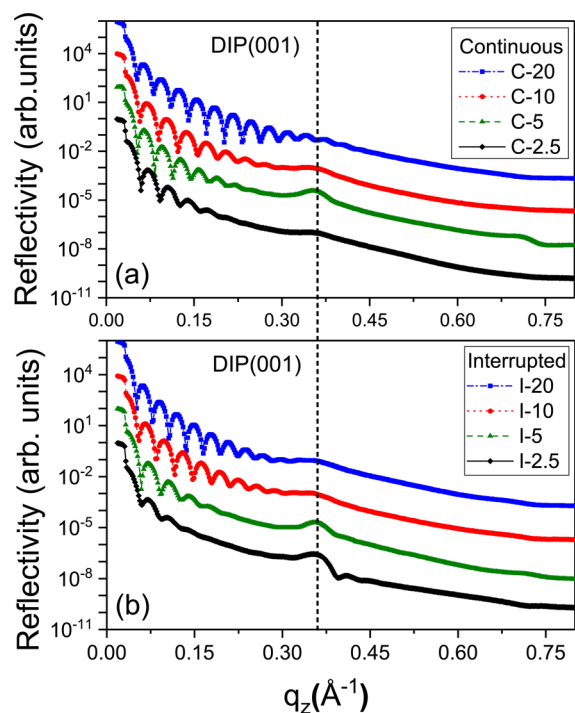


Figure 3. X-ray reflectivity of the equimolar DIP:C60 thin films. It is observed that (a) even the phase separating mixed thin film demonstrates an increase in the smoothness (or alternatively decrease in roughness) and decrease in the crystallinity as the growth rate r_{dep} changes from 2.5 to 20 Å/min. It is further seen that the same films, when codeposited with systematic interruptions (b), exhibit the same trend of the films being smoother and less crystalline as the growth rate increases. However, each of the films grown via interruptions (the growth and interruption times are variable for different growth rates) shows enhanced crystallinity compared to the film grown continuously at the same growth rate.

interruption at all different rates we observe the trend of decreasing crystallinity and increasing roughness. We speculate that since the flux is not very different between the samples C-5 and C-2.5, they form similar structure with similar crystallinity when grown continuously.

GIXD was also measured for the same films with different deposition procedures (Figure 4). The peak width and corresponding crystalline size estimated from GIXD measurements of thin films of similar thickness of the pure phases of DIP and C60 at the same growth temperature are roughly 200 Å, and 80 Å, respectively. In comparison to the pure phases, the mixed films have lower crystallite size of the constituent domains. Upon comparison of the films with the same rate, we observe that the films which were grown by interrupted growth clearly have more pronounced DIP reflections, at least for low r_{dep} , which indicates that the interruption in growth indeed enhances the in-plane crystallinity of the film, too. The C60 thin film is known to grow in a polycrystalline form (with a broad distribution of orientations)⁴ as opposed to DIP thin films which grow as strongly textured domains.²⁵ We do not observe any change in the width of the C60 peak (which is already broad due to codeposition of molecules) to infer about the C60 phase. We think that while the increase in crystallinity of the DIP domains increases the peak intensities and decreases the fwhm of the DIP diffraction peaks (as observed in the GIXD profiles) there is no obvious

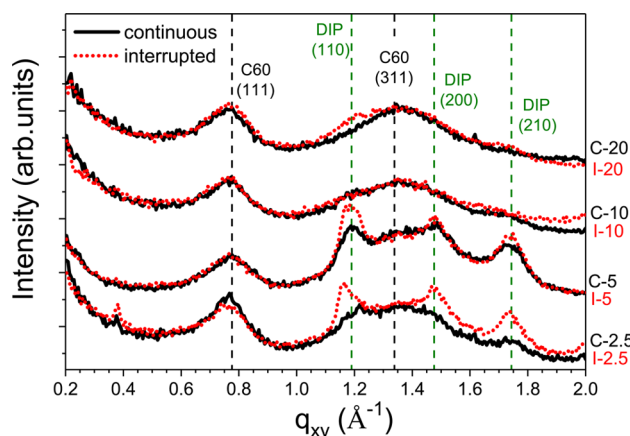


Figure 4. Grazing incidence X-ray diffraction (GIXD) data for the films with different growth rates and different pause times, grouped in pairs of continuous/interrupted growth with the same deposition rate (r_{dep}) during growth intervals. The prominent peaks can be assigned to DIP (110, 200, 210) and C60 (111 and 311) reflections. There are no additional peaks in the GIXD, confirming the fact that the mixtures actually phase separate. Additionally, it is seen that the DIP reflections are stronger for the interrupted growth scenario, particularly for the low r_{dep} . The higher growth rates (upper two pairs of curves) do not seem to affect the crystallinity appreciably. For both the growth modes (interrupted as well as continuous growth) the crystallinity decreases with the growth rates. Eventually, at higher rates, the crystallinity of both the growth modes appears to be very similar.

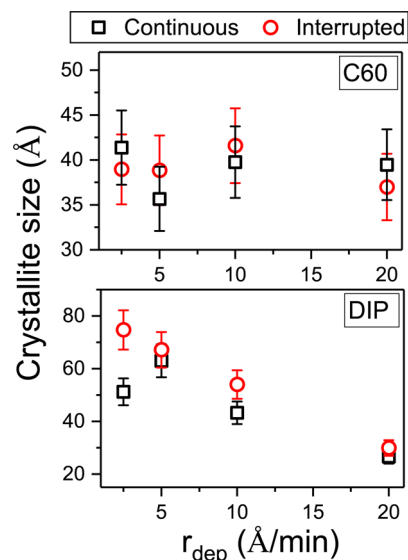


Figure 5. Crystallite size (d_{coh}) determined from the peak width of the GIXD profiles using the Scherrer formula for the different in-plane Bragg reflections for DIP as well as for C60 at different r_{dep} of 2.5, 5, 10, and 20 Å/min. While the crystallite size of C60 does not vary too much, the crystallite size of DIP shows a decreasing trend as a function of increasing r_{dep} . For the different growth modes, it is observed that the crystallinity of the DIP domains are mostly larger for the interrupted growth (compared to continuous growth), particularly at low r_{dep} , signifying enhanced phase separation for the DIP:C60 mixtures.

change perceived in the diffraction peaks for the polycrystalline C60 domains.

On the other hand, it was observed that for the high r_{dep} the difference between interrupted and continuous growth was negligible. This is corroborated by the XRR measurements

where we observed an appreciable enhancement of the out-of-plane crystallinity only for the low r_{dep} films. From the peak width of the known DIP and C60 Bragg reflections, we estimate the degree of phase separation by the crystallite sizes for the prominent peaks at different values of r_{dep} (Figure 5).

AFM data of the DIP:C60 equimolar mixture grown both continuously and by systematic interruption at all different growth rates (r_{dep}) of 2.5, 5, 7.5, 10, and 20 Å/min are shown in Figure 6. In comparison to continuous growth, for interrupted growth there is a larger number of presumably crystalline domains, which grow in a 3D like fashion. On comparing the domain size of C-2.5 and I-2.5 (refer to Figure S3 in the

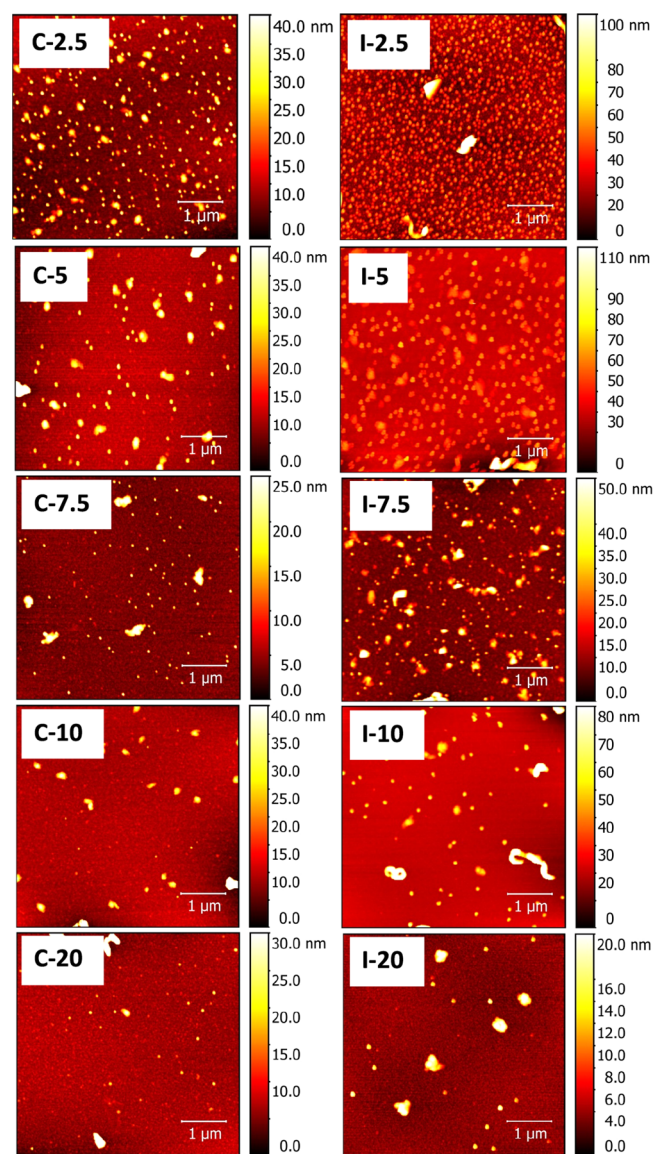


Figure 6. AFM images of the equimolar mixed films for continuous (C-2.5, C-5, C-7.5, C-10 and C-20) and interrupted growth (I-2.5, I-5, I-7.5, I-10, I-20) at growth rates (r_{dep}) of 2.5, 5, 7.5, 10, and 20 Å/min, respectively. This clearly demonstrates the trend of the decreasing surface coverage as r_{dep} increases for both continuous and interrupted growth modes. In general, the covered surface area of crystalline domains is significantly larger for interrupted growth compared to continuous growth. However, there are no significant differences observed in the surface coverage for both growth modes for larger values of r_{dep} .

Supporting Information) we see that the domain size is approximately 110 ± 10 nm for the continuous growth and 135 ± 22 nm for the interrupted growth, which is significantly larger than the average coherent in-plane island sizes determined from GIXD both for DIP and C60. Since GIXD is very sensitive to defect densities (like point defects and dislocations) in the scattering volume, we conclude that the defect density within one domain visible in AFM is still considerable and limits the determined coherent scattering island size. We assume, that the flat regions in between the domains are nearly amorphous which is also in agreement with our XRR and GIXD data. In continuous growth, the reduced surface coverage of these larger presumably crystalline domains of DIP results also in smoother films with less or no crystallinity in comparison to interrupted growth.

Since DIP is more crystalline than C60 in the mixtures and scales with deposition rate (Figure 5), we assume that the 3D domains in Figure 6 are mostly phase-separated crystalline DIP domains. The surface coverage of the crystalline DIP domains dependent on growth rate is shown in Figure 7. Data for the

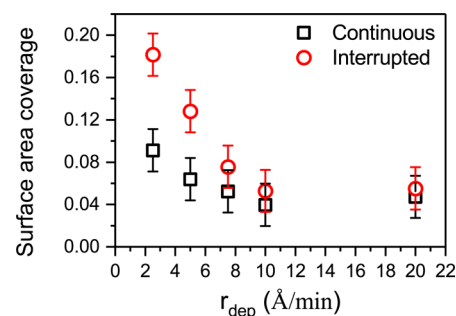


Figure 7. Surface area coverage of large domains as a function of the deposition rate (r_{dep}) determined from AFM data in Figure 6. The presence of large domains increases as r_{dep} decreases for both continuous as well as for interrupted growth.

surface coverage was extracted from different AFM images for all the different growth rates both for the continuous and the interrupted growth scenarios. Images were considered with sizes of both 10 and $5 \mu\text{m}^2$ for at least two to three different spots, and the average value of the coverage was plotted. Figure 6 clearly demonstrates the trend of the decreasing surface coverage as the growth rate increases for both continuous and interrupted growth modes. In general, the covered surface area of crystalline domains is significantly larger for interrupted growth compared to continuous growth. However, the differences in surface coverage for both growth modes decrease for larger r_{dep} . This observation is again in agreement with the crystalline coherent island size determined from GIXD.

We speculate that the large crystalline islands are pure domains which have been separated out from the nearly amorphous mixture by diffusion during the film growth. Interruptions in the growth process are expected to influence the morphology of the film if the interruption time scales are comparable to time scales which determine the processes shaping the film: surface diffusion, step diffusion, island formation and phase separation. Estimating the time scales of these processes for the studied mixture of DIP and C60 is a nontrivial problem. For films of pure materials, some information is available. Surface diffusion of free molecules appears to be a fast process. For C60 on C60 itself, all-atom simulations³⁶ estimate order-of-magnitude diffusion constants

D_s (at room temperature) of 10^{-6} cm²/s. Explicit numbers for DIP are not available but the values for PEN, which is of similar size and structure, is known in the literature. The aforementioned study³⁶ gives diffusion constants for PEN on PEN of about 10^{-4} cm²/s which are about a factor 10 higher than from a recent experiment.²³ Although the surface diffusion constant will be reduced for finite densities of molecules³⁶ (due to attractive interactions and therefore transient island formation), the typical time to traverse a lateral length such as the crystallite size (Figure 5), d_{coh}^2/D_s , is well below the millisecond range. Island formation, connected to step diffusion, is much slower. A study of the dewetting behavior of a pure first layer of DIP on nSiO at 130 °C showed a mass transport rate to the second layer of about 0.006 monolayers per minute.³⁷ If one assumes that transport of one tenth of a monolayer corresponds to an island formation time, one estimates about 16 min for the latter. The island formation time in a reference multilayer system of pure DIP at room temperature (as used in the present study) should be larger since both the lower temperature and the stronger interaction of DIP molecules with other DIP molecules compared with the substrate will decrease the interlayer transport. For a reference multilayer system of pure C60, it is known that a typical dewetting or island formation time is about 10 min (pure C60 deposited on closed C60 layers).³⁸ Both reference times are rather large on the time scale of the present investigations, and if DIP-C60 phase separation were dominated by island formation of the single components, one would not expect a noticeable difference between continuous and interrupted growth using the same growth rate. In the present study the slowest rate of 2.5 Å/min corresponds to about 6 min for depositing a thickness equivalent of a pure DIP layer. During that time three breaks of 1 min occur which is short compared to the island formation times in pure systems. Nevertheless, we observe enhanced out-of-plane crystallinity (Figure 3), larger DIP crystallite sizes (Figure 5) and increased surface coverage of crystalline domains (Figure 7). Thus, we conclude that a typical time scale for phase separation must be shorter, on the order of 1 min, to influence the rearrangements within one or two layers. The reason for such acceleration is not fully clear; contributions may arise from enhanced island formation rates of one component when the second component is present and the faster process of intralayer separation of DIP and C60 due to surface diffusion and the difference in interaction potentials between the species.

Phase separation in the DIP:C60 system is more complex than assumed in these estimates. We showed in a previous study⁶ that phase separation in thicker films became more effective in layers remote from the substrate. Thus, the typical time scale for phase separation will depend on height. Our results suggest that such height-dependent time scales can also be accessed by introducing a height dependence into the interruption protocol.

CONCLUSION

Equimolar mixtures of DIP and C60 were grown using different experimental conditions with a focus on the variation of the time averaged growth rate in the context of interrupted growth. The effect of systematic interruption of growth was studied and compared to the continuous growth scenario. X-ray scattering measurements XRR and GIXD were used to probe the out-of-plane and in-plane crystallinity of the thin films. AFM measurements were performed on the same set of samples

corroborating the finding that the crystallinity of the samples was higher for the lower rate of deposition as is usually observed for pristine organic thin films. On the basis of our measurements and analysis, we observe that phase separation mechanisms can be influenced by growth interruptions, in particular, if the deposition rates are already low. For high deposition rates, growth interruptions have little effect because based on the time scale considerations, the effect of the interruptions will be smeared out and gradually disappear for higher rates. It has also been mentioned that, due to the complex structure–property relationship, it is not always possible to single out any particular structural feature that might be useful in certain applications, but generally it is accepted in the community that a certain amount of roughness of the interface between the donor and the acceptor is favorable to enhance chances for exciton dissociation and thus organic photovoltaic device efficiency. Such information provides us a handle on the type of preparation conditions to tailor the length scale of phase separation in organic semiconductor thin film blends that lead to a specific type of growth and morphology preferred for a device or other applications in the field of organic electronics. Our results and comparison with time scales from simulation suggest the possibility of height-dependent time scales that may be further exploited to tailor the growth. Many other growth conditions can be investigated, for instance, the stoichiometry, functionalization of the substrate and thickness and time dependence of phase separation, but this would be beyond the scope of the present proof-of-concept study.

ASSOCIATED CONTENT

Supporting Information

The Supporting Information is available free of charge on the ACS Publications website at DOI: 10.1021/acs.jpcc.7b09637.

Details of the experimental schematic, fitted profiles of the grazing incidence X-ray diffraction measurements, and high-resolution AFM images of the equimolar mixed films, grown at a low rate of deposition for continuous and interrupted growth mode (PDF)

AUTHOR INFORMATION

Corresponding Author

*(R.B.) E-mail: rupakb@iitgn.ac.in.

ORCID

Rupak Banerjee: 0000-0002-1189-1502

Alexander Hinderhofer: 0000-0001-8152-6386

Notes

The authors declare no competing financial interest.

ACKNOWLEDGMENTS

This work is supported within the DFG/FNR INTER project by the Deutsche Forschungsgemeinschaft (DFG), Project No. OE 285/3-1 and SCHR 700/24-1. C.L. thanks the Carl-Zeiss-Stiftung for funding.

REFERENCES

- Brütting, W.; Adachi, C., Eds. *Physics of Organic Semiconductors*, 2nd ed.; Wiley VCH-Verlag: Weinheim, Germany, 2012.
- Forrest, S. R. The Path to Ubiquitous and Low-Cost Organic Electronic Appliances on Plastic. *Nature* **2004**, *428*, 911–918.
- Tang, C. W. Two-Layer Organic Photovoltaic Cell. *Appl. Phys. Lett.* **1986**, *48*, 183–185.

- (4) Hinderhofer, A.; Schreiber, F. Organic-Organic Heterostructures: Concepts and Applications. *ChemPhysChem* **2012**, *13*, 628–643.
- (5) Aufderheide, A.; Broch, K.; Novák, J.; Hinderhofer, A.; Nervo, R.; Gerlach, A.; Banerjee, R.; Schreiber, F. Mixing-Induced Anisotropic Correlations in Molecular Crystalline Systems. *Phys. Rev. Lett.* **2012**, *109*, 156102.
- (6) Banerjee, R.; Novák, J.; Frank, C.; Lorch, C.; Hinderhofer, A.; Gerlach, A.; Schreiber, F. Evidence for Kinetically Limited Thickness Dependent Phase Separation in Organic Thin Film Blends. *Phys. Rev. Lett.* **2013**, *110*, 185506.
- (7) Opitz, A.; Ecker, B.; Wagner, J.; Hinderhofer, A.; Schreiber, F.; Manara, J.; Pflaum, J.; Brütting, W. Mixed Crystalline Films of Co-Evaporated Hydrogen- and Fluorine-Terminated Phthalocyanines and Their Application in Photovoltaic Devices. *Org. Electron.* **2009**, *10*, 1259–1267.
- (8) Belova, V.; Beyer, P.; Meister, E.; Linderl, T.; Halbich, M.-U.; Gerhard, M.; Schmidt, S.; Zechel, T.; Meisel, T.; Generalov, A. V.; et al. Evidence for Anisotropic Electronic Coupling of Charge Transfer States in Weakly Interacting Organic Semiconductor Mixtures. *J. Am. Chem. Soc.* **2017**, *139*, 8474–8486.
- (9) Goiri, E.; Matena, M.; El-Sayed, A.; Lobo-Checa, J.; Borghetti, P.; Rogero, C.; Detlefs, B.; Duvernay, J.; Ortega, J.; et al. de Oteyza, Self-Assembly of Bicomponent Molecular Monolayers: Adsorption Height Changes and Their Consequences. *Phys. Rev. Lett.* **2014**, *112*, 117602.
- (10) Rivnay, J.; Mannsfeld, S. C. B.; Miller, C. E.; Salleo, A.; Toney, M. F. Quantitative Determination of Organic Semiconductor Microstructure from the Molecular to Device Scale. *Chem. Rev.* **2012**, *112*, 5488–5519.
- (11) Deibel, C.; Dyakonov, V. Polymer-Fullerene Bulk Heterojunction Solar Cells. *Rep. Prog. Phys.* **2010**, *73*, 096401.
- (12) Dennler, G.; Scharber, M. C.; Brabec, C. J. Polymer-Fullerene Bulk-Heterojunction Solar Cells. *Adv. Mater.* **2009**, *21*, 1323–1338.
- (13) Liscio, F.; Albonetti, C.; Broch, K.; Shehu, A.; Quiroga, S. D.; Ferlauto, L.; Frank, C.; Kowarik, S.; Nervo, R.; Gerlach, A.; et al. Molecular Reorganization in Organic Field-Effect Transistors and Its Effect on Two-Dimensional Charge Transport Pathways. *ACS Nano* **2013**, *7*, 1257–1264.
- (14) Wagner, J.; Gruber, M.; Hinderhofer, A.; Wilke, A.; Bröker, B.; Frisch, J.; Amsalem, P.; Vollmer, A.; Opitz, A.; Koch, N.; et al. High Fill Factor and Open Circuit Voltage in Organic Photovoltaic Cells with Diindenoperylene as Donor Material. *Adv. Funct. Mater.* **2010**, *20*, 4295–4303.
- (15) Gruber, M.; Rawolle, M.; Wagner, J.; Magerl, D.; Hörmann, U.; Perlich, J.; Roth, S. V.; Opitz, A.; Schreiber, F.; Müller-Buschbaum, P.; et al. Correlating Structure and Morphology to Device Performance of Molecular Organic Donor-Acceptor Photovoltaic Cells Based on Diindenoperylene (DIP) and C₆₀. *Adv. Energy Mater.* **2013**, *3*, 1075–1083.
- (16) Hörmann, U.; Lorch, C.; Hinderhofer, A.; Gerlach, A.; Gruber, M.; Kraus, J.; Sykora, B.; Grob, S.; Linderl, T.; Wilke, A.; et al. V_{OC} From a Morphology Point of View: The Influence of Molecular Orientation on the Open Circuit Voltage of Organic Planar Heterojunction Solar Cells. *J. Phys. Chem. C* **2014**, *118*, 26462–26470.
- (17) Zheng, Y. Q.; Wang, C.; Yu, J. L.; Yang, F.; Wei, B.; Lin, Y.; Li, X. F.; Adachi, C. Diindenoperylene (DIP) Concentration Dependent Photovoltaic Performance and Dielectric Properties for Mixed Heterojunctions. *Synth. Met.* **2017**, *233*, 35–40.
- (18) Michely, T.; Krug, J. *Islands, Mounds, and Atoms. Patterns and Processes in Crystal Growth Far from Equilibrium*; Springer: Berlin, 2004.
- (19) Pimpinelli, A.; Villain, J. *Physics of Crystal Growth*; Cambridge University Press: Cambridge, U.K., 1998.
- (20) Schreiber, F. Organic Molecular Beam Deposition: Growth Studies Beyond the First Monolayer. *phys. stat. sol. (a)* **2004**, *201*, 1037–1054.
- (21) Nahm, R. K.; Bullen, H. J.; Suh, T.; Engstrom, J. R. Faster Is Smoother and So Is Lower Temperature: The Curious Case of Thin Film Growth of Tetracene on SiO₂. *J. Phys. Chem. C* **2017**, *121*, 8464–8472.
- (22) Nahm, R. K.; Engstrom, J. R. Unexpected Effects of the Rate of Deposition on the Mode of Growth and Morphology of Thin Films of Tetracene Grown on SiO₂. *J. Phys. Chem. C* **2016**, *120*, 7183–7191.
- (23) Rotter, P.; Lechner, B. A. J.; Morherr, A.; Chisnall, D. M.; Ward, D. J.; Jardine, A. P.; Ellis, J.; Allison, W.; Eckhardt, B.; Witte, G. Coupling Between Diffusion and Orientation of Pentacene Molecules on an Organic Surface. *Nat. Mater.* **2016**, *15*, 397–400.
- (24) Zykov, A.; Bommel, S.; Wolf, C.; Pithan, L.; Weber, C.; Beyer, P.; Santoro, G.; Rabe, J. P.; Kowarik, S. Diffusion and Nucleation in Multilayer Growth of PTCDI-C8 Studied With In Situ X-ray Growth Oscillations and Real-Time Small Angle X-Ray Scattering. *J. Chem. Phys.* **2017**, *146*, 052803.
- (25) Kowarik, S. Thin Film Growth Studies Using Time-Resolved X-Ray Scattering. *J. Phys.: Condens. Matter* **2017**, *29*, 043003.
- (26) Nicklin, C. Capturing Surface Processes. *Science* **2014**, *343*, 739–740.
- (27) Lorch, C.; Frank, H.; Banerjee, R.; Hinderhofer, A.; Gerlach, A.; Li Destri, G.; Schreiber, F. Controlling Length-Scales of The Phase Separation to Optimize Organic Semiconductor Blends. *Appl. Phys. Lett.* **2015**, *107*, 201903.
- (28) Lorch, C.; Novák, J.; Banerjee, R.; Weimer, S.; Dieterle, J.; Frank, C.; Hinderhofer, A.; Gerlach, A.; Carla, F.; Schreiber, F. Influence of C₆₀ Co-Deposition on the Growth Kinetics of Diindenoperylene From Rapid Roughening to Layer-By-Layer Growth in Blended Organic Films. *J. Chem. Phys.* **2017**, *146*, 052807.
- (29) Schünemann, C.; Wynands, D.; Wilde, L.; Hein, M.; Pfützner, S.; Elschner, C.; Eichhorn, K.-J.; Leo, K.; Riede, M. Phase Separation Analysis of Bulk Heterojunctions in Small-Molecule Organic Solar Cells using Zinc-Phthalocyanine and C₆₀. *Phys. Rev. B: Condens. Matter Phys.* **2012**, *85*, 245314.
- (30) Breuer, T.; Witte, G. Thermally Activated Intermixture in Pentacene-Perfluoropentacene Heterostructures. *J. Chem. Phys.* **2013**, *138*, 114901.
- (31) Tu, C.; Miller, R.; Wilson, B.; Petroff, P.; Harris, T.; Kopf, R.; Sputz, S.; Lamont, M. Properties of (Al,Ga)As/GaAs Heterostructures Grown by Molecular Beam Epitaxy with Growth Interruption. *J. Cryst. Growth* **1987**, *81*, 159–163.
- (32) Fukunaga, T.; Kobayashi, K. L. I.; Nakashima, H. Photoluminescence from AlGaAs-GaAs Single Quantum Wells with Growth Interrupted Heterointerfaces Grown by Molecular Beam Epitaxy. *Jpn. J. Appl. Phys.* **1985**, *24*, L510.
- (33) Tanaka, M.; Sakaki, H.; Yoshino, J. Atomic-Scale Structures of Top and Bottom Heterointerfaces in GaAsAl_xGa_{1-x}As (x = 0.2–1) Quantum Wells Prepared by Molecular Beam Epitaxy with Growth Interruption. *Jpn. J. Appl. Phys.* **1986**, *25*, L155.
- (34) Ide, T.; Yamashita, A.; Mizutani, T. Direct Observation of the Growth-Interruption Effect for Molecular-Beam-Epitaxy Growth on GaAs(001) by Scanning Tunneling Microscopy. *Phys. Rev. B: Condens. Matter Phys.* **1992**, *46*, 1905–1908.
- (35) Kowarik, S.; Gerlach, A.; Sellner, S.; Schreiber, F.; Cavalcanti, L.; Konovalov, O. Real-Time Observation of Structural and Orientational Transitions during Growth of Organic Thin Films. *Phys. Rev. Lett.* **2006**, *96*, 125504.
- (36) Cantrell, R.; Clancy, P. A Computational Study of Surface Diffusion of C₆₀ on Pentacene. *Surf. Sci.* **2008**, *602*, 3499–3505.
- (37) Kowarik, S.; Gerlach, A.; Sellner, S.; Cavalcanti, L.; Schreiber, F. Dewetting in an Organic Semiconductor Thin Film Observed in Real-Time. *Adv. Eng. Mater.* **2009**, *11*, 291–294.
- (38) Bommel, S.; Kleppmann, N.; Weber, C.; Spranger, H.; Schäfer, P.; Novák, J.; Roth, S.; Schreiber, F.; Klapp, S. H.; Kowarik, S. Unravelling the Multilayer Growth of the Fullerene C₆₀ in Real Time. *Nat. Commun.* **2014**, *5*, 5388.